Supporting Information

Rational Design of Lead-Free $CsCu_2I_3$@g-C_3N_4 Composite for Efficient Energy Storage and Sustainable Catalysis

Montu Gogoi[a], Deepshikha Roy[a], Jita Morang[a], Nilakshi Dutta[a], Tarun Kumar Sahu[b], Diganta Sarma[a] and Kalyanjyoti Deori[a]*

[a]*KD's 'NAME' (NanoMat&Energy) Lab, Department of Chemistry, Dibrugarh University, Dibrugarh-786004, Assam, India*

[b]*Indian Institute of Technology Indore, Department of Chemistry, Madhya Pradesh-453552, India*

Email: kalchemdu@gmail.com; kalchemdu@dibru.ac.in

Additional Experimental Details:

The specific capacitance from the CV curve was calculated by using **equation S1**:

$$C = \frac{1}{m \times s \times \Delta V} \int I(V) dV \tag{S1}$$

Where, $\int I(V) dV$= integral area of CV curve, m = mass of the active material, s = scan rate (mV/s), and ΔV = potential difference.

The specific capacitance was calculated from the galvanostatic charge-discharge (GCD) curve using the following **equation S2**:

$$C = \frac{I \Delta t}{m \Delta V} \tag{S2}$$

Where, C= specific capacitance (F/g), I = applied current (A), Δt = discharge time (s), m = mass of the active material, and ΔV = potential difference.

The energy density was evaluated using the **equation S3**:

$$E = \frac{1}{2 \times 3.6} CV_2 \tag{S3}$$

Where, E= energy density (Wh/Kg), C = specific capacitance (F/g), and V = operating voltage (V).

The power density was determined by using **equation S4**:

$$P = \frac{3600 \times E}{\Delta t} \tag{S4}$$

Where, P = power density (W/Kg), E = energy density (Wh/Kg), and Δt = discharge time (s).

Table S1 Kinetic parameters derived from the analysis of emission decay of the as-synthesized samples.

Sample	A_1	τ_1	A_2	τ_2	A_3	τ_3	τ_{avg} (ns)
CCI	656.076	114.52	259.129	244.35	-	-	**151.2798**
CCI-CN	299.778	36.91	485.7	171.01	-	-	**119.8307**
CN	5704.766	0.8	3800.438	3.17	608.752	11.90	**2.36**

The average lifetime was calculated using the following **equation S5**:

$$\tau avg = \frac{\tau 1A1}{A1 + A2 + A3} + \frac{\tau 2A2}{A1 + A2 + A3} + \frac{\tau 3A3}{A1 + A2 + A3}$$

(S5)

Where, A_1, A_2, and A_3 are pre-exponential values for luminescence lifetimes τ_1, τ_2, and τ_3, respectively.

Table S2 Screening of optimized conditions for the photo-hydration of benzonitriles to corresponding benzamide derivatives.[a]

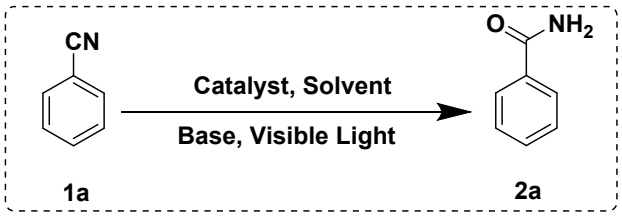

Entry	Deviation from the standard conditions	Yield (%)
		2a
1	2 h	80
2	Without light	NR
3	Without CCI-CN	NR
4	CCI (Instead of CCI-CN)	70
5	CN (Instead of CCI-CN)	40
6	MeOH (Instead of *i*-PrOH)	65
7	EtOH (Instead of *i*-PrOH)	70
8	H_2O (Instead of *i*-PrOH)	40
9	20 W Visible light	40
10	NaOH (Instead of KOH)	85
11	Na_2CO_3 (Instead of KOH)	45
12	K_2CO_3 (Instead of KOH)	NR
13	CCI-CN (5 mg)	81
14	CuI (Instead of CCI-CN)	40
15	Without light (5 h)	NR
16	None*	97

[a]**Reaction conditions**: Benzonitrile (0.5 mmol), KOH (1 mmol), and CCI-CN (10 mg) were stirred in *i*-PrOH (2.5 ml) for 3 h under 250 W visible-light irradiation. N.R.=no reaction. *None= the standard reaction condition with no change.

Table S3 Screening of optimized conditions for the synthesis of quinazolin-4(*3H*)-ones.[b]

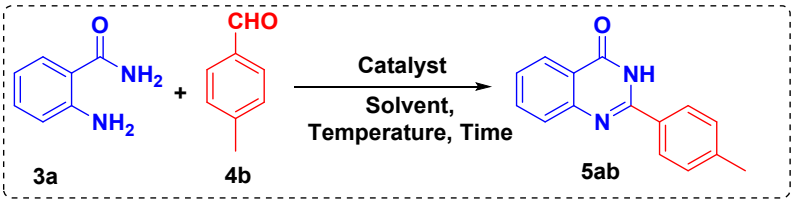

Entry	Deviation from the standard conditions	Yield (%)
		5ab
1	2 h	70
2	Without Solvent	NR
3	Without CCI-CN	NR
4	H_2O (Instead of DMSO), 6 h	50
5	Methanol (Instead of DMSO), 6 h	60
6	Ethyl Acetate (Instead of DMSO), 6 h	40
7	DMSO, 6 h	98
8	RT, 6 h	NR
9	RT, 12 h	NR
10	RT, 18 h	NR
11	40 ºC, 6 h	50
12	50 ºC, 6 h	50
13	60 ºC, 6 h	50
14	CCI (Instead of CCI-CN)	75
15	CN (Instead of CCI-CN)	Trace
16	CuI (Instead of CCI-CN)	40
17	None*	98

[b]**Reaction conditions:** 2-aminobenzamide (0.1 mmol, 1 equivalent), 4-methylbenzaldehyde (0.12 mmol, 1.2 equivalent), and CCI-CN (10 mg) were stirred in DMSO (1 ml) at 80 ºC for 4 h. N.R.=no reaction. *None= the standard reaction condition with no change.

Table S4 Comparison study of a few reported works on benzonitrile hydration with this work.

Entry	Catalyst	*hv*	Temperature	Time (h)	Yield (%)	Reference
1	Ni-Complex	-	70 ºC	6	91	1
2	Mn-Complex	-	100 ºC	18	90	2
3	Os-Complex	-	120 ºC	4	91	3
4	$PdCl_2$+As_2O_3	-	60 ºC	12	54	4
5	Mn-PNP Complex	-	92 ºC	24	85	5
6	Ru@MnO_2	-	60 ºC	6	94	6
7	**CCI-CN**	**250 W Visible light**	**RT**	**3**	**97**	**This work**

Table S5 Comparison study of a few reported works on quinazoline-4(*3H*)-one synthesis with this work.

Entry	Catalyst	Solvent	Additives	Temperature	Time (h)	Yield (%)	Reference
1	Mo(VI)-Complex	EtOH	H_2O_2	80 ºC	6	82	7
2	$H_3PW_{12}O_{40}$	EtOH:H_2O	-	100 ºC	4.5	75	8
3	$Cu(OAc)_2$	PhMe	Oxone	100 ºC	10	78	9
4	Fe_3O_4-CND	H_2O	TBHP	90 ºC	14	82	10
5	Ni(II)-Complex	EtOH	-	78 ºC	6	81	11
6	MSPHS ionic liquid@SiO_2	EtOH:H_2O	TBHP	120 ºC	24	83.2	12
7	**CCI-CN**	**DMSO**	**-**	**80 ºC**	**4**	**98**	**This work**

Table S6 Evaluation of the electrochemical performance of few previously reported perovskite-based electrodes.

Entry	Supercapacitor	Specific Capacitance, C_{sp}	Power Density	Reference
1	$CsPbBr_3$	121 F/g at 1 A/g	625 W/Kg	13
2	La_2FeMnO_6	10.58 mF/g at 0.9 mA/g	435.33 W/Kg	14
3	Y_2NiMnO_6	77.76 F/g at 30 mA/g	4.32 W/Kg	15
4	$CH_3NH_3PbBr_3$	54.36 F/g at 5 mV/s	225 W/Kg	16
5	$(4\text{-FBA})_2MA_{n-1}Pb_nI_{3n+1}$ (Quasi-2D)	8.67 F/g at 5 mV/s	109 W/Kg	17
6	$La_{1-x}Sr_xMnO_3$	102 F/g at 1 A/g	120 W/Kg	18
7	**CCI-CN**	**149.4 F/g at 1.16 A/g**	**992 W/Kg**	**This work**

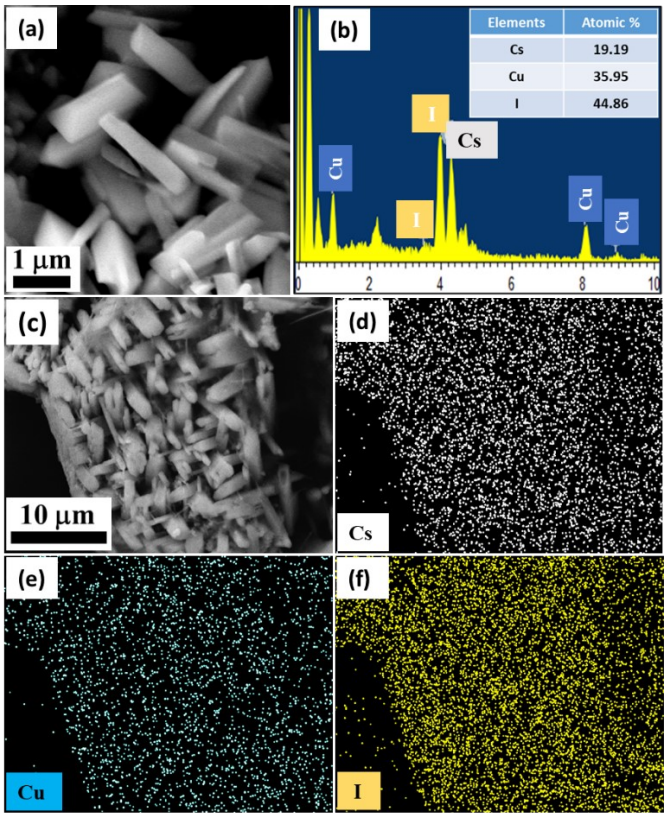

Fig. S1 EDX spectra and elemental mapping of CCI.

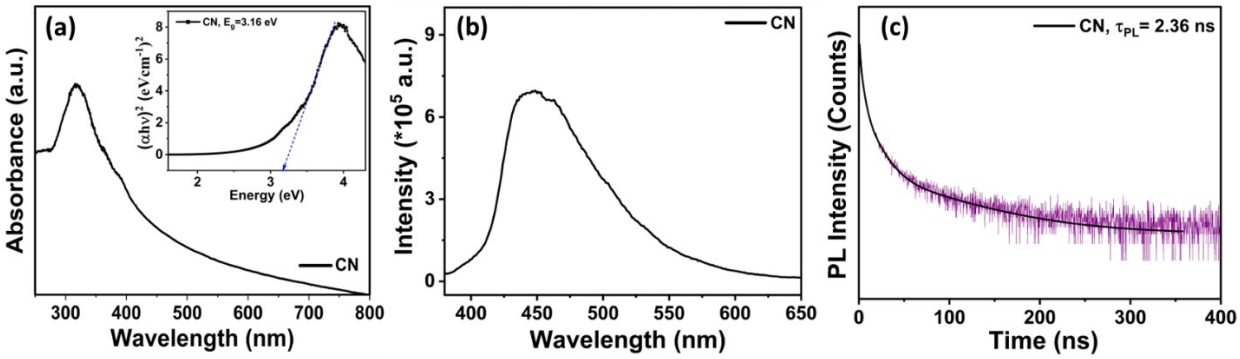

Fig. S2 (a) Absorption spectra of CN. The inset shows the corresponding bandgap energy of the sample using Tauc's plot, (b) PL emission spectra of CN, and (c) Time-resolved PL decay curves of CN.

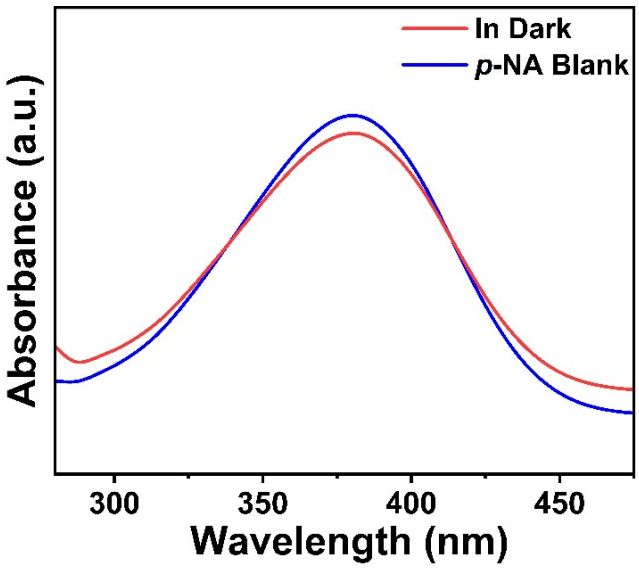

Fig. S3 Time-dependent optical absorption spectra after stirring without photocatalyst (blank) and in dark with photocatalyst for *para*-nitroaniline reduction.

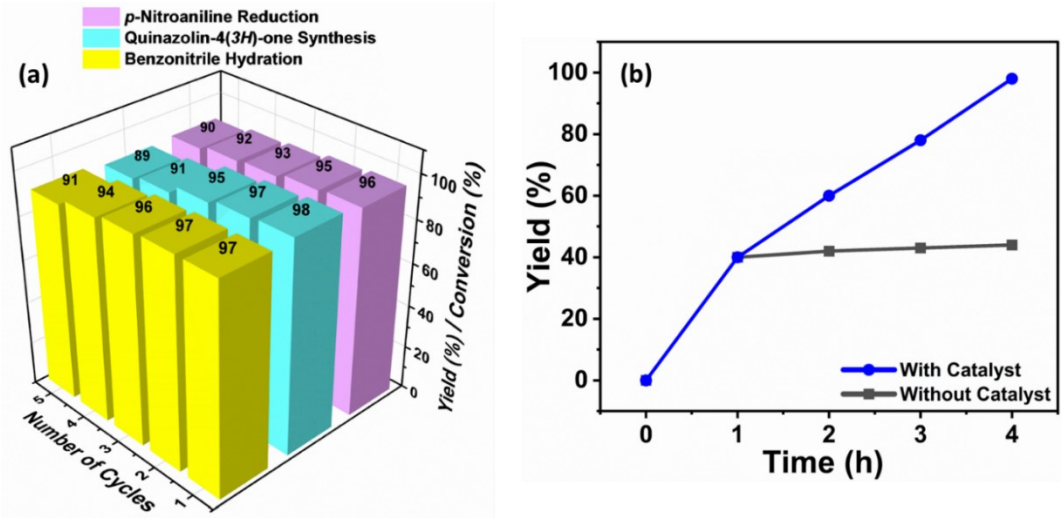

Fig. S4 (a) Recyclability test of CCI-CN, (b) hot-injection test for synthesis of quinazolin-4(*3H*)-one.

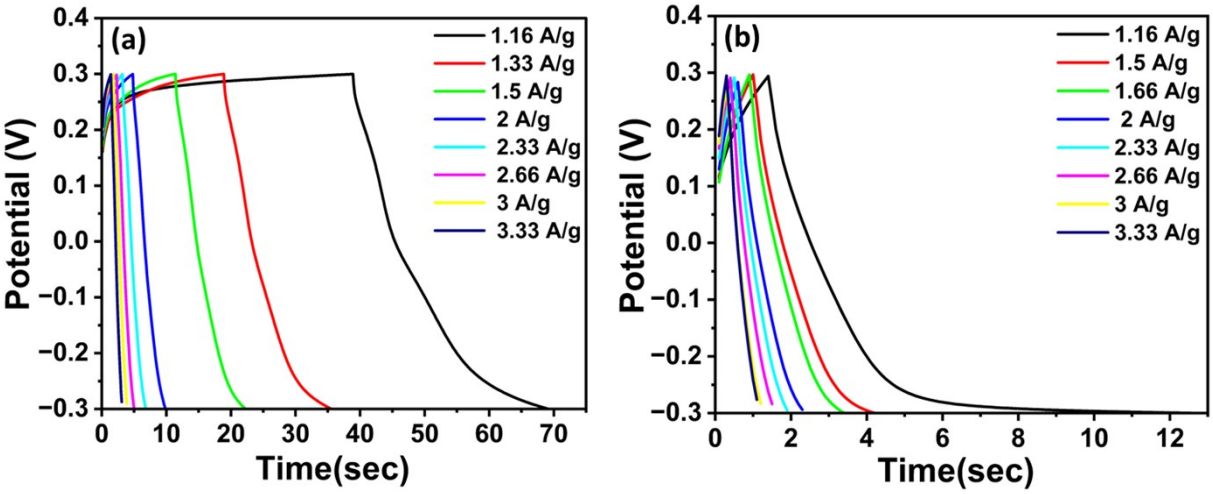

Fig. S5 Galvanostatic charge-discharge (GCD) curves at different current densities for (a) CCI, and (b) CN.

Analytical data of representative compound

Benzamide (2a)

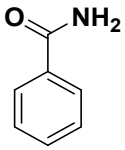

^{1}H NMR (500 MHz, DMSO) δ 7.97 (s, 2H), 7.88 (d, *J* = 7.3 Hz, 2H), 7.51 (t, *J* = 7.2 Hz, 1H), 7.44 (t, *J* = 7.4 Hz, 2H).

^{13}C NMR (126 MHz, DMSO) δ 168.25 (s), 134.61 (s), 131.55 (s), 128.54 (s), 127.79 (s).

4-methylbenzamide (2d)

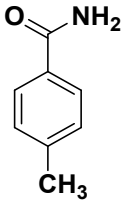

^{1}H NMR (500 MHz, DMSO) δ 7.89 (s, 2H), 7.77 (d, *J* = 7.5 Hz, 2H), 7.24 (d, *J* = 7.7 Hz, 2H), 2.34 (s, 3H).

^{13}C NMR (126 MHz, DMSO) δ 168.36 (s), 141.62 (s), 132.07 (s), 129.31 (s), 128.08 (s), 21.52 (s).

2-(p-tolyl)quinazolin-4(*3H*)-one (5ab)

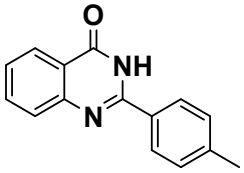

^{1}H NMR (500 MHz, DMSO) δ 12.43 (s, 1H), 8.12 (d, *J* = 6.9 Hz, 1H), 8.07 (d, *J* = 8.2 Hz, 2H), 7.78 (t, *J* = 7.6 Hz, 1H), 7.69 (d, *J* = 8.0 Hz, 1H), 7.46 (t, *J* = 7.5 Hz, 1H), 7.32 (d, *J* = 8.1 Hz, 2H), 2.35 (s, 3H).

^{13}C NMR (125 MHz, DMSO) δ 162.62, 152.59, 149.02, 141.67, 134.77, 130.18, 129.42, 127.94, 126.61, 126.10, 121.11, 21.21.

MS (ESI) m/z: $[M+H]^+$ calcd. for $C_{15}H_{12}N_2OH$ 237.09; Found 237.13.

2-(4-fluorophenyl)quinazolin-4(*3H*)-one (5ac)

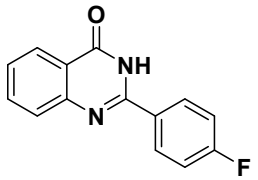

^{1}H NMR (500 MHz, DMSO) δ 12.70 (s, 1H), 8.39 (d, J = 15.0 Hz, 2H), 8.30 (d, J = 5 Hz, 1H), 7.97 (t, J = 10.0 Hz, 1H), 7.87 (d, J = 10.0 Hz, 1H), 7.66 (t, J = 5.0 Hz, 1H), 7.53 (t, J = 5.0 Hz, 2H).

^{13}C NMR (125 MHz, DMSO) δ 164.38 (d, *J* = 249.5 Hz), 162.55 (s), 151.70 (s), 149.00 (s), 134.96 (s), 130.70 (d, *J* = 30 Hz), 127.80 (s), 126.94 (s), 126.19 (s), 121.23 (s), 115.96 (d, *J* =3.9 Hz).

MS (ESI) m/z: $[M+H]^+$ calcd. for $C_{14}H_9FN_2OH$ 241.06; Found 241.09.

2-(4-chlorophenyl)quinazolin-4(*3H*)-one (5ad)

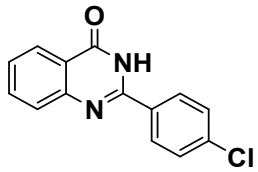

^{1}H NMR (500 MHz, DMSO) δ 12.67 (s, 1H), 8.26 (d, *J* = 8.5 Hz, 1H), 8.22 (d, *J* = 7.7 Hz, 1H), 7.91 (t, *J* = 7.6 Hz, 1H), 7.81 (d, *J* = 8.1 Hz, 2H), 7.69 (d, *J* = 8.5 Hz, 2H), 7.60 (t, *J* = 7.4 Hz, 1H).

^{13}C NMR (125 MHz, DMSO) δ 162.9, 152.15, 149.21, 136.95, 135.33, 132.25, 130.30, 129.34, 126.56, 121.66.

MS (ESI) m/z: $[M+H]^+$ calcd. for $C_{14}H_9ClN_2OH$ 257.06; Found 257.03.

2-(4-methoxyphenyl)quinazolin-4(*3H*)-one (5ag)

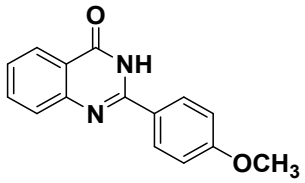

^{1}H NMR (500 MHz, DMSO) δ 12.33 (s, 1H), 8.12 (d, *J* = 8.9 Hz, 2H), 8.06 (d, *J* = 7.9 Hz, 1H), 7.73 (t, *J* = 6.9 Hz, 1H), 7.63 (d, *J* = 8.0 Hz, 1H), 7.40 (t, *J* = 7.9 Hz, 1H), 7.00 (d, *J* = 8.9 Hz, 2H), 3.77 (s, 3H).

^{13}C NMR (125 MHz, DMSO) δ 162.75, 162.27, 152.29, 149.33, 134.91, 131.74, 129.89, 127.67, 126.50, 126.24, 125.21, 121.11, 114.25, 55.91.

MS (ESI) m/z: $[M+H]^+$ calcd. for $C_{15}H_{12}N_2O_2H$ 253.08; Found 253.11.

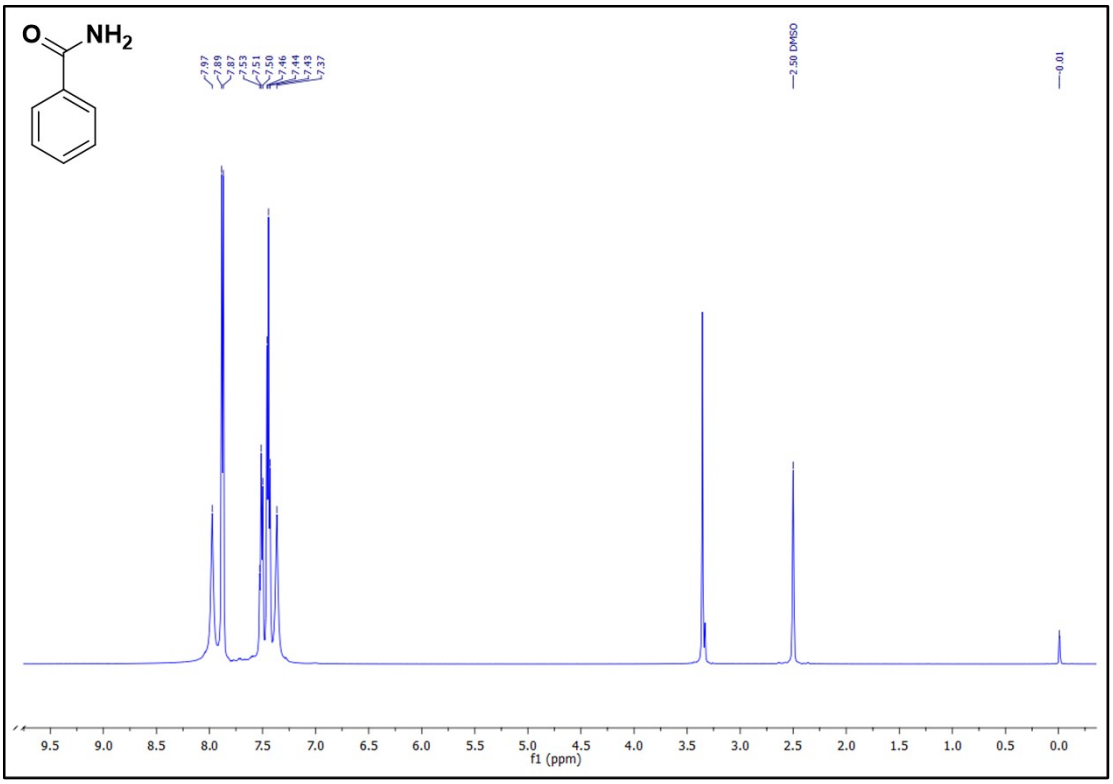

Fig. S6 ^{1}H NMR spectrum of Benzamide (2a)

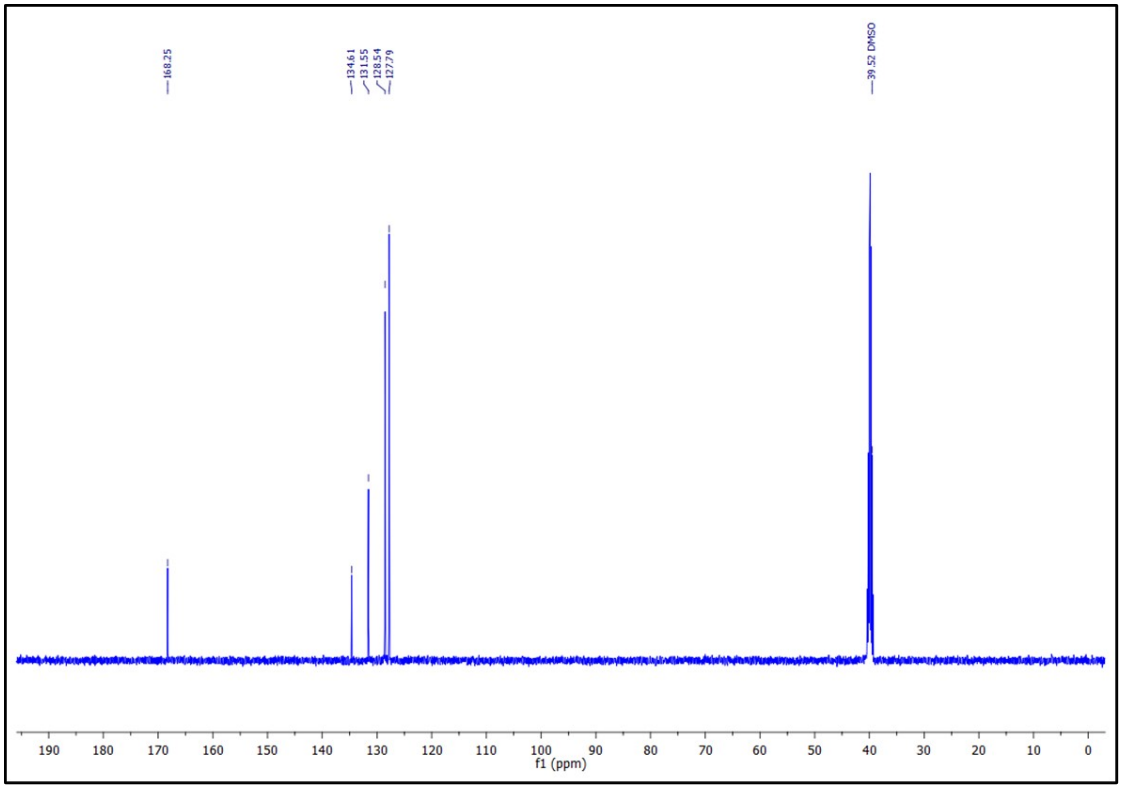

Fig. S7 ^{13}C NMR spectrum of Benzamide (2a)

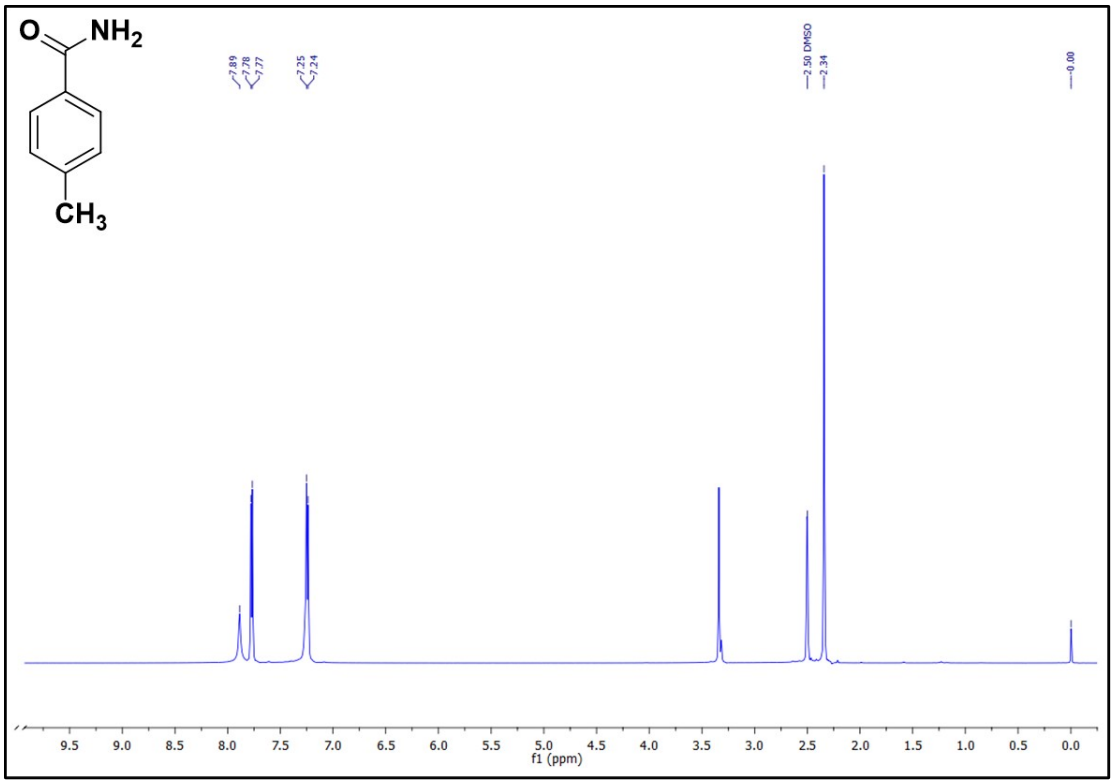

Fig. S8 ^{1}H NMR spectrum of 4-methylbenzamide (2d)

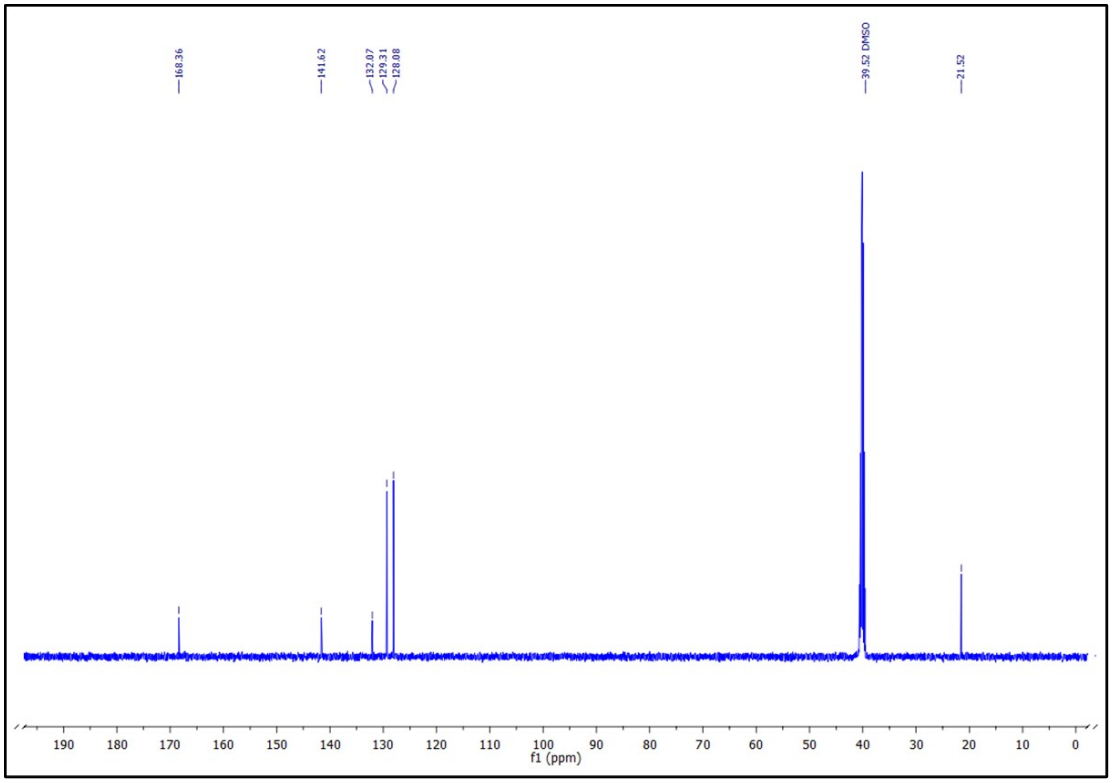

Fig. S9 ^{13}C NMR spectrum of 4-methylbenzamide (2d)

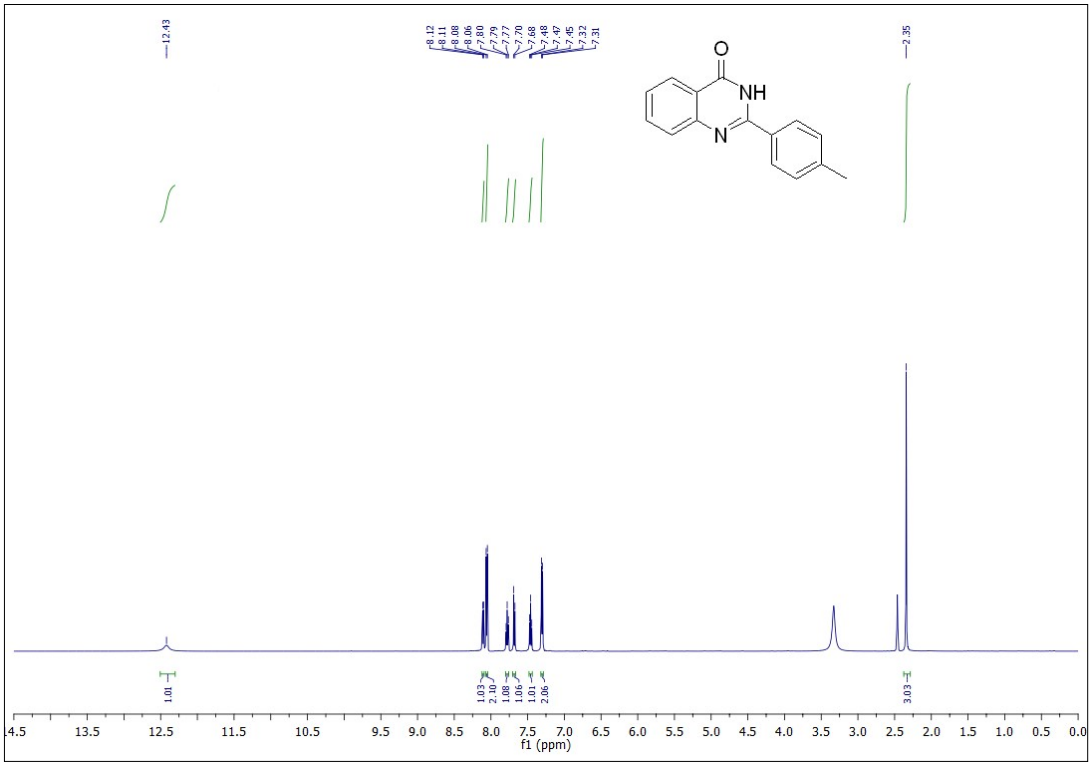

Fig. S10 ^{1}H NMR spectrum of 2-(p-tolyl)quinazolin-4(*3H*)-one (5ab)

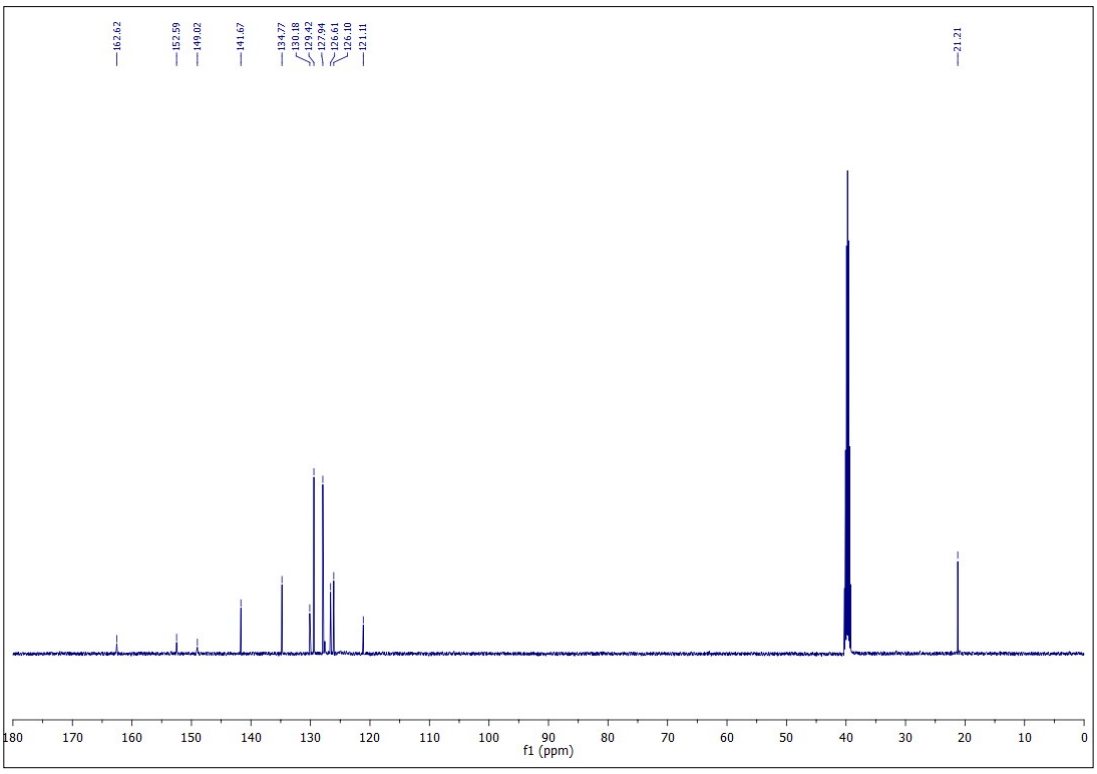

Fig. S11 ^{13}C NMR spectrum of 2-(p-tolyl)quinazolin-4(*3H*)-one (5ab)

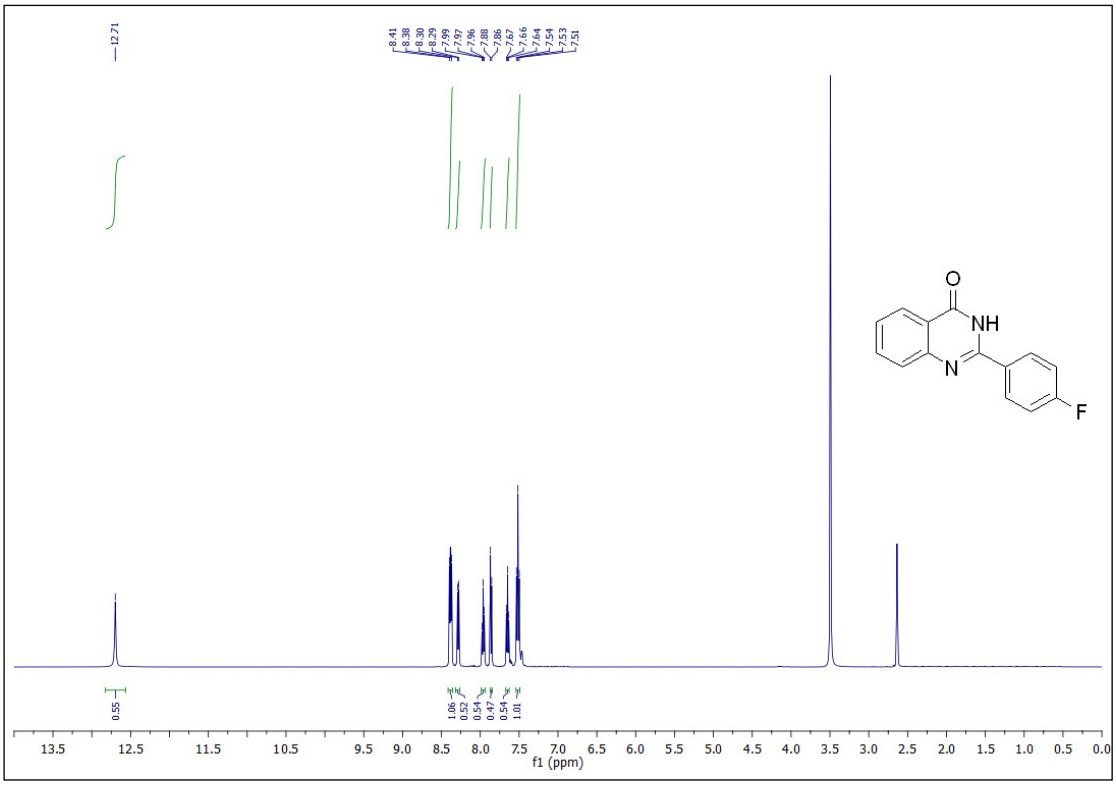

Fig. S12 ^{1}H NMR spectrum 2-(4-fluorophenyl)quinazolin-4(*3H*)-one (5ac)

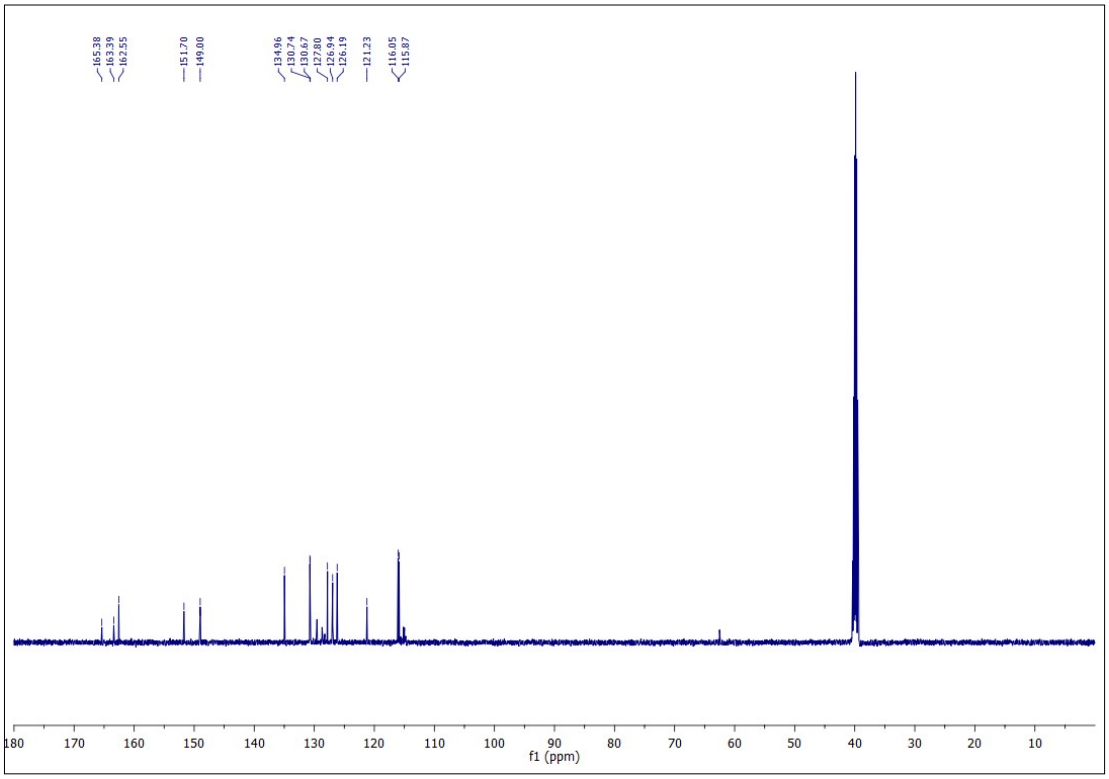

Fig. S13 ^{13}C NMR spectrum 2-(4-fluorophenyl)quinazolin-4(*3H*)-one (5ac)

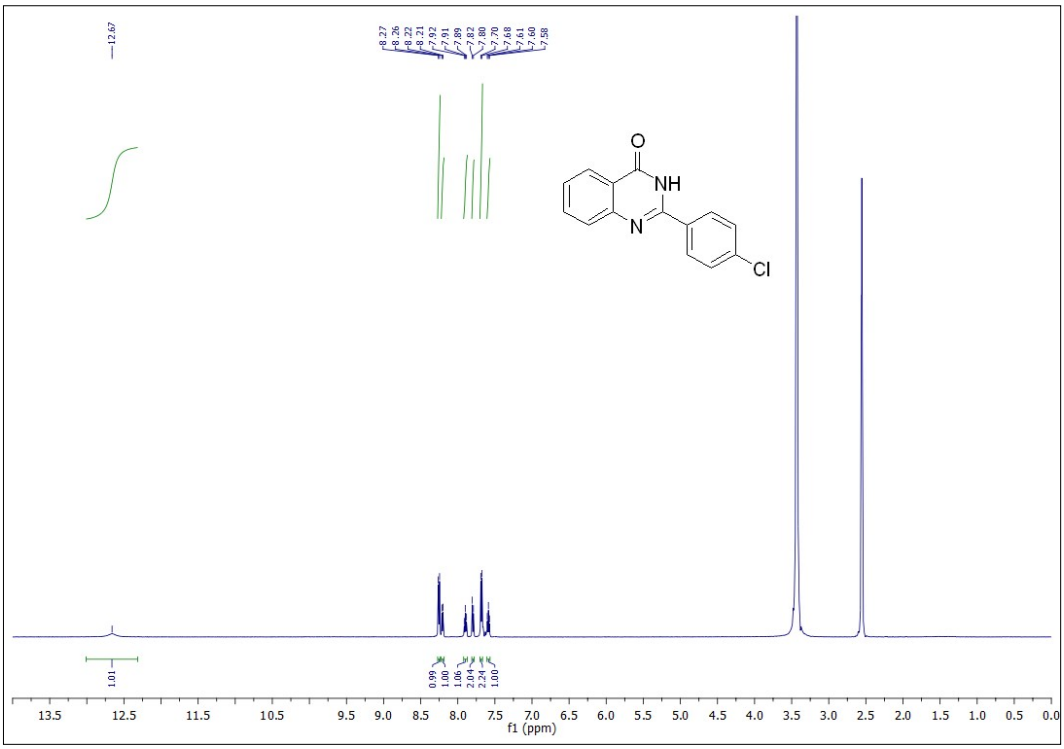

Fig. S14 ^{1}H NMR spectrum 2-(4-chlorophenyl)quinazolin-4(*3H*)-one (5ad)

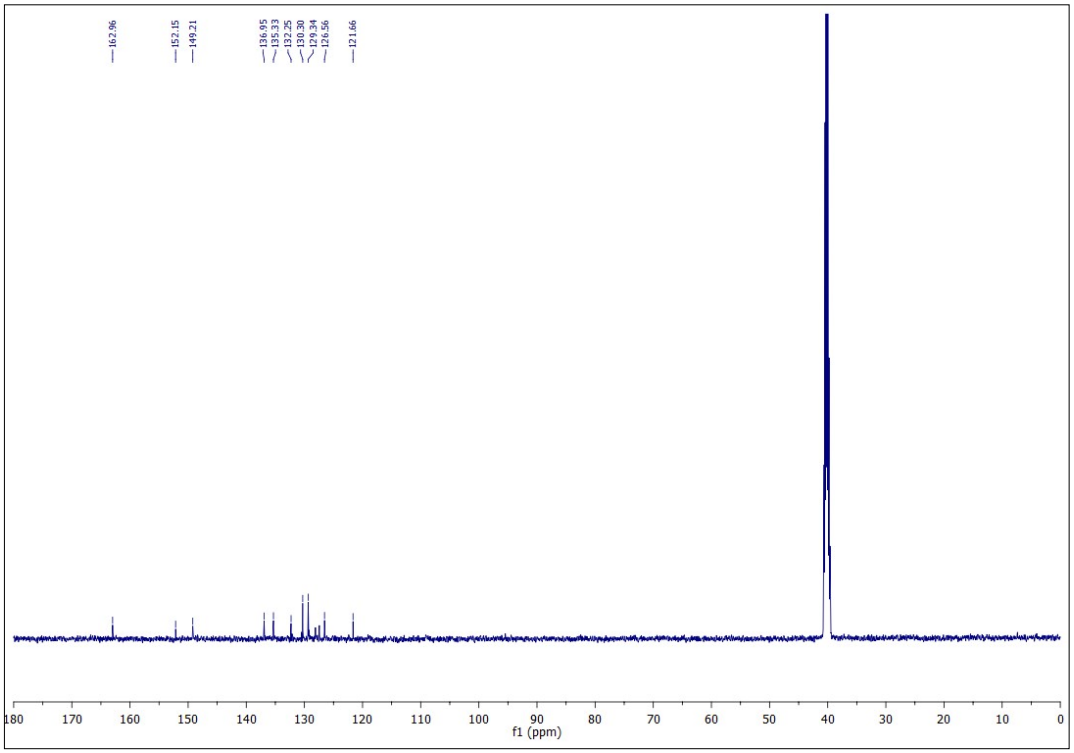

Fig. S15 ^{13}C NMR spectrum 2-(4-chlorophenyl)quinazolin-4(*3H*)-one (5ad)

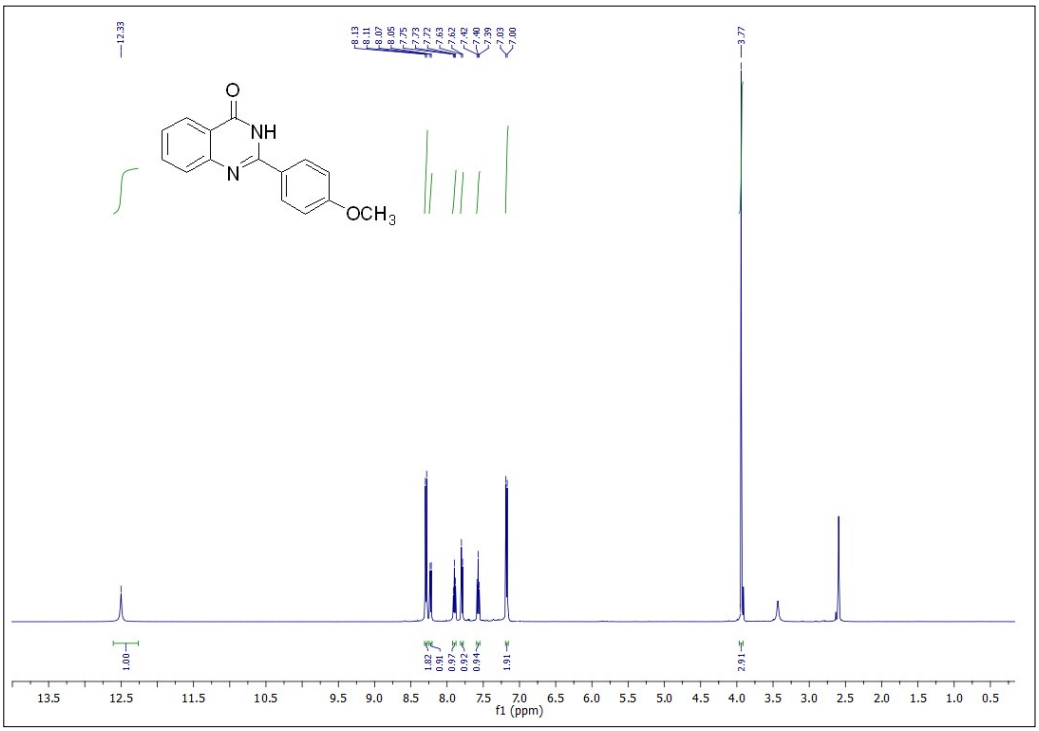

Fig. S16 ^{1}H spectrum 2-(4-methoxyphenyl)quinazolin-4(*3H*)-one (5ag)

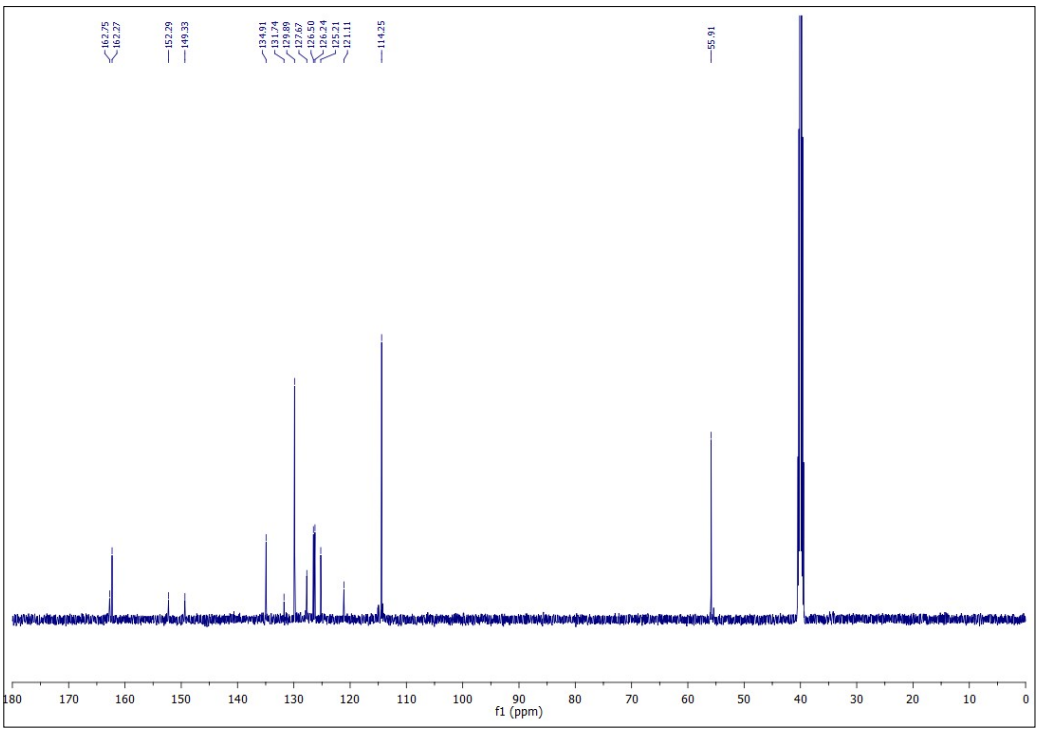

Fig. S17 ^{13}C NMR spectrum 2-(4-methoxyphenyl)quinazolin-4(*3H*)-one (5ag)

References

1 K. Singh, A. Sarbajna, I. Dutta, P. Pandey and J. K. Bera, Hemilability-Driven Water Activation: A Ni^{II} Catalyst for Base-Free Hydration of Nitriles to Amides, *Chem. Eur. J.*, 2017, **23**, 7761–7771.

2 J. A. Garduño, A. Arévalo, M. Flores-Alamo and J. J. García, Mn(i) Organometallics Containing the $^{i}Pr_2P(CH_2)_2P^{i}Pr_2$ Ligand for the Catalytic Hydration of Aromatic Nitriles, *Catal. Sci. Technol.*, 2018, **8**, 2606–2616.

3 M. L. Buil, V. Cadierno, M. A. Esteruelas, J. Gimeno, J. Herrero, S. Izquierdo and E. Oñate, Selective Hydration of Nitriles to Amides Promoted by an Os–NHC Catalyst: Formation and X-Ray Characterization of K_2-Amidate Intermediates, *Organometallics*, 2012, **31**, 6861–6867.

4 D. Cirri, T. Marzo and A. Pratesi, An Unprecedented Palladium-Arsenic Catalytic Cycle for Nitriles Hydration, *Front. Chem.*, 2023, **11**.

5 Q.-Q. Zhou, Y.-Q. Zou, S. Kar, Y. Diskin-Posner, Y. Ben-David and D. Milstein, Manganese-Pincer-Catalyzed Nitrile Hydration, α-Deuteration, and α-Deuterated Amide Formation via Metal Ligand Cooperation, *ACS Catal.*, 2021, **11**, 10239–10245.

6 M. A. Hussain, E. J. Choi, A. Maqbool, M. Atif, H. Zeb, J. Yeo, J.-A. Yu, Y.-H. Cho, M. Noh and J. W. Kim, An Efficient Hydration of Nitriles with Ruthenium-Supported Heterogeneous Catalyst in Water under Moderate Conditions, *J. Ind. Eng. Chem.*, 2021, **99**, 187–195.

7 M. Feng, Q. Yan, L. Yang, Y. Ye, G. Liu and W. Wang, Selective Synthesis of 2-Substituted 2,3-Dihydroquinazolin-4(1H)-Ones and Quinazolin-4(3H)-Ones Catalyzed by Schiff Base Dioxomolybdenum(VI) Complex, *Int. J. Chem. Kinet.*, 2023, **55**, 119–128.

8 M. Tajbakhsh, R. Hosseinzadeh, P. Rezaee and M. Tajbakhsh, $H_3PW_{12}O_{40}$ Catalyzed Synthesis of Benzoxazine and Quinazoline in Aqueous Media, *Chin. J. Catal.*, 2014, **35**, 58–65.

9 S. K. Bera, M. Irfan and A. Porcheddu, An Efficient Strategy for Quinazolinone and Benzimidazole Synthesis Using Microwave-Assisted Copper-Catalyzed Aerobic Oxidation of Amines, *ChemCatChem*, 2025, **17**, 202401813.

10 R. Varala, V. Seema, M. Amanullah and M. M. Alam, Recent Advances in TBHP-Promoted Heterocyclic Ring Construction via Annulation/Cyclization, *J. Heterocycl. Chem.*, 2024, **61**, 1269–1298.

11 U. P. Singh, S. Sharma and A. Malik, Nickel(II) Complex Anchored on MCM-41, a Reusable Catalyst for the Synthesis of Benzimidazole and Quinazolinone, *J. Coord. Chem.*, 2022, **75**, 2111–2123.

12 T. T. T. Huynh, T. T. Nguyen and P. H. Tran, An Efficient and Green Synthesis of 2-Phenylquinazolin-4(3)-Ones Using Brønsted Acidic Ionic Liquid Grafted onto Silica, *J. Chem. Technol. Biotechnol.*, 2023, **98**, 555–565.

13 S. Thakur, T. Paul, S. Maiti and K. K. Chattopadhyay, All-Inorganic $CsPbBr_3$ Perovskite as Potential Electrode Material for Symmetric Supercapacitor, *Solid State Sci.*, 2021, **122**, 106769.

14 A. Shereef, A. K. Jose, J. Kunjumon, P. A. Aleena, M. A. Anu, W. Akram, R. P. Jebin, T. S. Xavier, T. Maity and D. Sajan, Study on Preparation, Magnetic Properties and Performance of Electrochemical Supercapacitor Based on La_2FeMnO_6 Double Perovskite for Energy Storage Applications and Their Charge Storage Mechanism, *Adv. Powder Technol.*, 2024, **35**, 104618.

15 M. Alam, K. Karmakar, M. Pal and K. Mandal, Electrochemical Supercapacitor Based on Double Perovskite Y_2NiMnO_6 Nanowires, *RSC Adv.*, 2016, **6**, 114722–114726.

16 R. Kumar, P. S. Shukla, G. D. Varma and M. Bag, Synthesis of Porous Electrode from $CH_3NH_3PbBr_3$ Single Crystal for Efficient Supercapacitor Application: Role of Morphology on the Charge Storage and Stability, *Electrochim. Acta*, 2021, **398**, 139344.

17 M. K. Rao, M. Saquib, M. Selvakumar, M. M.G., S. Paramasivam, N. S. Prabhu, S. Senthilkumar and S. D. Kamath, Quasi 2D Ruddlesden–Popper Perovskite Thin Film Electrode for Supercapacitor Application: Role of Diffusion and Capacitive Process in Charge Storage Mechanism, *FlatChem*, 2023, **41**, 100527.

18 X. Lang, H. Mo, X. Hu and H. Tian, Supercapacitor Performance of Perovskite $La_{1-x}Sr_xMnO_3$, *Dalton Trans.*, 2017, **46**, 13720–13730.